Eur. Phys. J. B **11**, 401–406 (1999)

THE EUROPEAN PHYSICAL JOURNAL B

EDP Sciences

Weak ferromagnetism in $LaMnO_3$

V. Skumryev[1], F. Ott[1,a], J.M.D. Coey[1], A. Anane[2,b], J.-P. Renard[2], L. Pinsard-Gaudart[3], and A. Revcolevschi[3]

[1] Physics Department, Trinity College, Dublin 2, Ireland
[2] Institut d'Électronique Fondamentale, Université Paris-Sud, 91405 Orsay Cedex, France
[3] Laboratoire de Chimie des Solides, Université Paris-Sud, 91405 Orsay Cedex, France

Received 8 January 1999

Abstract. The magnetic properties of $(La_{1-x}Sr_x)MnO_3$ crystals have been studied. The ac susceptibility $\chi = \chi' + i\chi''$ has been measured at frequencies ranging from 10 Hz to 1 000 Hz. The $x = 0.25$ crystal shows a typical ferromagnetic behaviour with a dimensionless SI susceptibility of 6 below $T_c = 350$ K limited by the demagnetizing field. Both $x = 0$ and $x = 0.06$ crystals show very sharp peaks in χ' and χ'' at the Néel points, 139 K and 135 K respectively. This is quite unlike the usual behaviour of an antiferromagnet. Magnetization measurements on an untwinned single crystal of $LaMnO_3$ show a weak moment of 0.18 μ_B/Mn at 4.2 K which is directed along the c axis. The origin of this canted antiferromagnetic structure is discussed in terms of anisotropy and of Dzyaloshinskii-Moriya interaction. It is concluded that anistropy is insufficient to explain the canted antiferromagnetism.

PACS. 75.25.+z Spin arrangements in magnetically ordered materials (including neutron and spin-polarized electron studies, synchrotron-source X-ray scattering, etc.) – 75.50.Ee Antiferromagnetics – 75.40.Gb Dynamic properties (dynamic susceptibility, spin waves, spin diffusion, dynamic scaling, etc.)

1 Introduction

Stoichiometric $LaMnO_3$ contains Mn^{3+} ions arranged in an A_y-type planar antiferromagnetic structure which consists of oppositely aligned ferromagnetic {001} planes [1]. The early neutron diffraction studies [2,3] indicated that the arrangement in the *ab* plane is ferromagnetic (spins in the plane with the moment parallel to the orthorhombic *b*-axis in the Pbnm space group) but successive planes are coupled antiferromagnetically. In-plane and intraplane exchange parameters have been determined by inelastic neutron scattering [4,5]: the intraplane ferromagnetic exchange constant is $J_1 = 9.6$ K and the interplane antiferromagnetic exchange constant is $J_2 = -6.8$ K. Matsumoto [6] was the first to attribute the weak moment measured in polycrystalline $LaMnO_3$ at 77 K to the Dzyaloshinskii-Moriya (D-M) interaction [7,8]. However there has been no study so far of the weak ferromagnetism of $LaMnO_3$ on single crystals.

It is well known that it is possible to dope $LaMnO_3$ with divalent cation so as to obtain mixed valence manganese compounds. Doping with Sr to give $(La_{1-x}Sr_x)MnO_3$ results in a complicated magnetic phase diagram with successive transitions from an insulating antiferromagnetic ($0 < x < 0.1$) to an insulating ferromagnetic ($0.1 < x < 0.16$) and then to a metallic ferromagnetic state ($0.16 < x < 0.4$) [1]. This is due to competition between superexchange and double exchange interactions. The ferromagnetic order is mediated through the double exchange interaction between the Mn^{3+} and Mn^{4+} ions as described by Zener [9]. This interaction is related to the resonant tunnelling exchange of an electron between Mn ions accross the Mn-O-Mn bond. There are also some recent suggestions that materials with $x \ll 0.1$ may be segregated into a nanoscale mixture of antiferromagnetic and ferromagnetic phases [10].

Here we report the ac susceptibility and magnetization of crystals of pure $LaMnO_3$. We include some susceptibility data on crystals of $(La_{1-x}Sr_x)MnO_3$ with $x > 0$ for comparison. For $LaMnO_3$, we have been able to measure an untwinned crystal in the three principal directions, as well as crystals of $LaMnO_3$, $(La_{0.94}Sr_{0.06})MnO_3$ and $(La_{0.75}Sr_{0.25})MnO_3$ which were twinned.

2 Experimental methods

The crystals were grown by a floating zone method in an image furnace [11]. The $LaMnO_3$ crystal structure was indexed on an orthorhombic cell with $a = 0.554$ nm, $b = 0.575$ nm and $c = 0.769$ nm. Most of the orthorhombic crystals exhibit twinning which is related to the fact that

[a] *Present address*: Laboratoire Léon Brillouin, CEA/CNRS, Centre d'Études de Saclay, 91191 Gif-sur-Yvette Cedex, France.
e-mail: `fott@spec.saclay.cea.fr`
[b] *Present address*: MARTECH, P.O. Box 4000, Florida State University, Tallahassee, Florida 32306, USA.

the crystal structure is very close to a cubic cell ($a \approx b \approx c/\sqrt{2} \approx 0.55$ nm). There are two possible types of twinning [4]: the orientation of the c axis can lie along the [100], [010] or [001] directions of the pseudo-cubic cell; the a and b axes can be interchanged, c remaining in the same direction. This gives rise to 6 possible orientations of the crystal. X-ray diffraction from the plane perpendicular to the growth axis, shows that [h00], [0h0] and [$hh2h$] peaks are present at the same time with a preponderance of [0h0] texture. The $(La_{0.94}Sr_{0.06})MnO_3$ crystal has been indexed on an orthorhombic cell with $a = 0.553$ nm, $b = 0.558$ nm and $c = 0.791$ nm. $(La_{0.75}Sr_{0.25})MnO_3$ has been indexed on a cubic cell with $a = 0.549$ nm. In the case of $LaMnO_3$, it was possible to find a small untwinned region of the ingot and most of the measurements were made on this sample.

The absolute value of the real χ' and imaginary χ'' components of the ac susceptibility were obtained in a field of 80 A/m and 800 A/m at frequencies ranging from 10 Hz to 1 000 Hz, in the temperature range 4–400 K using a home-made mutual induction bridge. The volume susceptibility was calculated using the room temperature X-ray densities of 6.58 g/cm^3, 6.50 g/cm^3, and 6.28 g/cm^3 for $LaMnO_3$, $(La_{0.94}Sr_{0.06})MnO_3$ and $(La_{0.75}Sr_{0.25})MnO_3$ respectively. The untwinned sample was a cube approximately 1 mm in size. The other samples were disks cut perpendicular to the growth direction ($\phi = 5.5$ mm, $h = 1.5$ mm for $LaMnO_3$; $\phi = 3$ mm and $h = 1$ mm for Sr doped samples. In order to minimise the demagnetizing effect, the field was applied in the plane of the disks. These disk planes do not contain the ferromagnetic ab plane. For $(La_{0.94}Sr_{0.06})MnO_3$ and $(La_{0.75}Sr_{0.25})MnO_3$ crystals the direction perpendicular to the disk is the [100] direction.

Magnetization as a function of field and temperature were measured using a SQUID magnetometer in a superconducting magnet with a field of up to 7.5 T applied along the principal directions.

3 Results

The magnetization of $LaMnO_3$ measured along the three crystallographic directions is shown in Figure 1. It is seen that the weak moment is directed along c, and its value is 0.18 μ_B/Mn ($M = 27.6$ kA/m). The field obtained by extrapolating to saturation the magnetization curve measured along a is $\mu_0 H = 2\mu_0 H_e = 80$ T. We obtain $\mu_0 H_e = 40$ T which is in good agreement with the value deduced from J_2.

Measurements in high fields on the same crystal show a spin-flop when the field is directed along b which occurs in 17 T at 4.2 K [12]. Popov *et al.* report that the spin-flop transition investigated by magnetostriction measurements occurs in a twinned crystal at 20 T [13].

Temperature dependence of the external susceptibility for $LaMnO_3$ is shown in Figure 2. External susceptibility refers to the susceptibility uncorrected for demagnetizing effects. χ' shows a very sharp peak at $T = 138$ K along

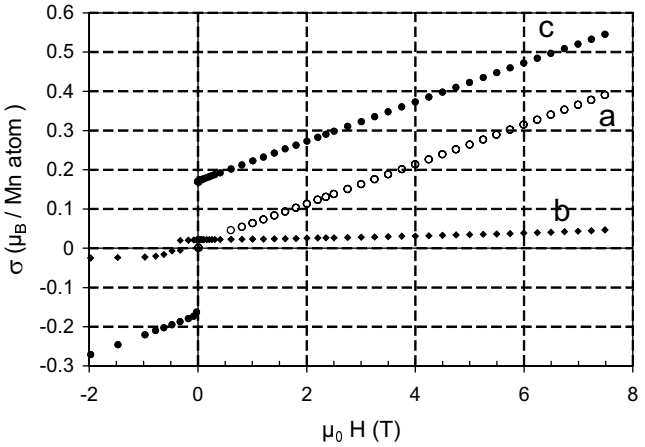

Fig. 1. Magnetization curves at 20 K for a single crystal of $LaMnO_3$ along the three orthorhombic axis.

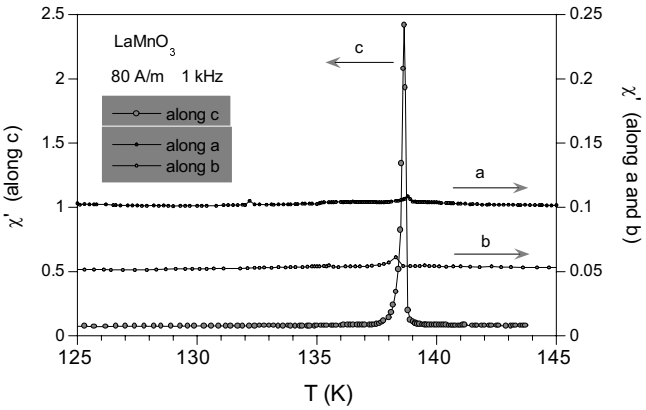

Fig. 2. ac-susceptibility of a single crystal of $LaMnO_3$ along the three orthorhombic axis in a field of 80 A/m at 1 kHz.

the c direction (Fig. 2). The magnitude of the real component of the susceptibility reaches 2.5 and the half width is about 0.2 K at 1 kHz (the demagnetizing limit of the susceptibility for a cubic sample is 3). There are no other peculiarities down to 4.2 K, the lowest temperature of our measurements. Along the a and b axes no significant anomaly is observed. A 1° misorientation of the crystal axes can explain the tiny peaks. The imaginary component χ'' exhibits a sharp maximum at the temperature where χ' peaks, with an amplitude comparable to the real component (Fig. 3). Both χ' and χ'' peaks broaden and shift slightly to lower temperatures when the ac field is increased from 80 A/m to 800 A/m (Fig. 3). Figure 4 shows a field-cooled and zero-field-cooled measurement in a dc field of 2 700 A/m. When the temperature is increased, the magnetization shows a sharp increase at 133 K where the coercive field of the material becomes smaller than the applied field. We expect that the coercivity falls to 800 A/m and 80 A/m at 136.5 K and 137.8 K respectively. The frequency effects are very large as can be seen in Figure 5. The peaks in both χ' and χ'' broaden with decreasing frequency (from 1 kHz to 10 Hz). The effects are slightly different on the real and imaginary parts of the susceptibility. In the real part, the peak simply broadens below

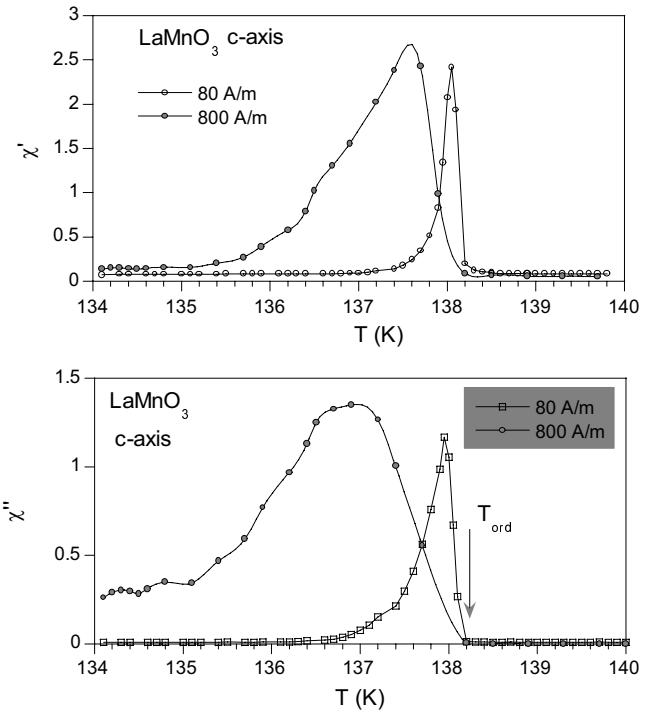

Fig. 3. Real and imaginary parts of the susceptibility of a single crystal of the $LaMnO_3$ measured along c in a 80 A/m field at 1 kHz.

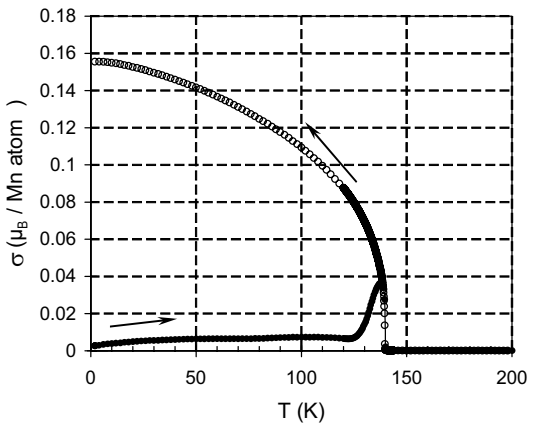

Fig. 4. Field and zero field cooled magnetization of a single crystal of $LaMnO_3$ measured along c in a field of 1 700 A/m.

T_N without any change in its amplitude. In the imaginary part however the peak not only broadens but also shifts to lower temperatures and its amplitude decreases. The onset of the losses remains at 138.2 K, which is identified as the Néel temperature.

The susceptibility of the twinned $LaMnO_3$ and $(La_{0.94}Sr_{0.06})MnO_3$ crystals is very similar (Fig. 6) except that the amplitude of the peaks is now much smaller than the factor 1/3 expected from the twinning (0.1 compared to $0.33 \times 2.5 = 0.8$). A possible explanation is that the coercivity in the twinned crystal could be much larger

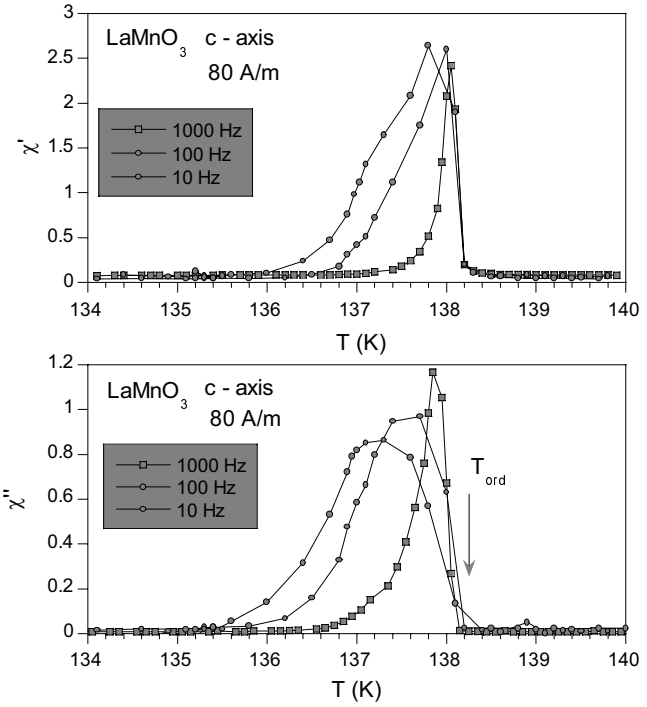

Fig. 5. Frequency dependence of the susceptibility of a single crystal of $LaMnO_3$ measured along c.

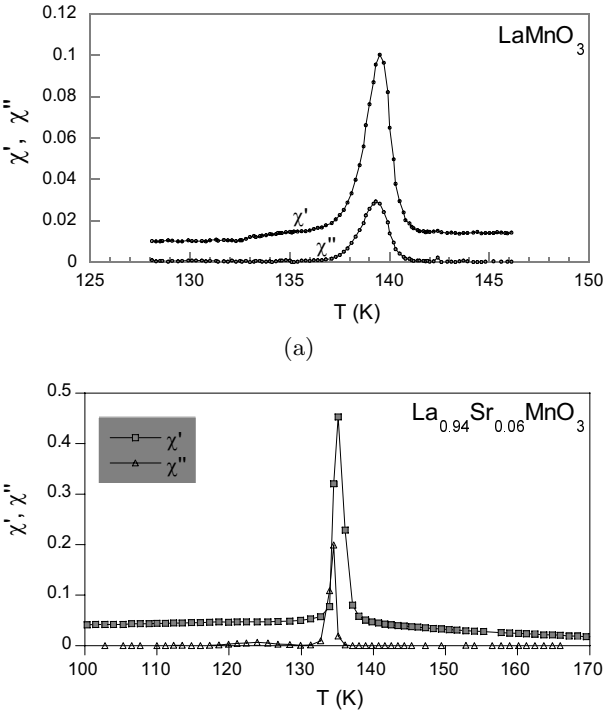

Fig. 6. ac-susceptibility of twinned crystals of $LaMnO_3$ (a) and $(La_{0.94}Sr_{0.06}MnO_3)$ (b) measured in 80 A/m at 1 kHz.

than in the single crystal because domain walls will tend to be pinned at the twin boundaries.

For the ferromagnetic $x = 0.25$ crystal, χ' increases rapidly at $T_c = 350$ K to saturate at the demagnetizing

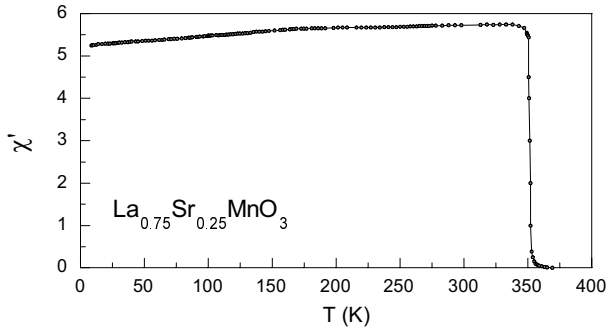

Fig. 7. ac-susceptibility of a crystal of ($La_{0.75}Sr_{0.25}MnO_3$) measured in 80 A/m at 1 kHz.

field limit of 6 corresponding to the value of the demagnetizing factor $N = 0.17$ given by the crystal shape (Fig. 7). It slightly decreases at low temperature. The measured value of χ'' below T_c is of order 10^{-2}. The temperature dependence of the susceptibility for the $x = 0.25$ crystal is typical of a soft ferromagnetic material. The rapid increase of χ' at 350 K is related to the establishment of ferromagnetic order at the Curie temperature.

4 Discussion

The observed sharp peak in the $\chi(T)$ data at T_N for $x = 0$ and $x = 0.06$ crystals is very different from the behaviour expected for normal antiferromagnetic order where the susceptibility increases smoothly with decreasing temperature towards a cusp at the Néel point T_N. Below T_N the susceptibility perpendicular to the antiferromagnetic axis is almost constant while the parallel susceptibility vanishes as T tends to zero. Only a cusp is detected in the susceptibility at T_N in either component.

However the situation in weak ferromagnets is usually quite different. If the canting is due to the crystal field interaction of the type DS_z^2, the susceptibility is expected to diverge on the scale of $\varepsilon_0 = (T_N - T_0)/T_N$ where $\varepsilon_0 = (D/\sum |J_i|)^2$ and T_0 is the temperature where the susceptibility begins to diverge; if the canting is due to the D-M interaction $\mathcal{D}(\mathbf{S}_i \times \mathbf{S}_j)$, the susceptibility diverges on the scale of $\varepsilon_0 = (\mathcal{D}/\sum |J_i|)^2$ [7]. Experimentally sharp peaks in χ' and large values of χ'' are often found near T_N for weak ferromagnets [14–19]. In our case we find that $\varepsilon_0 = 10^{-3}$, hence D or $\mathcal{D}$ is of order 1 K.

This begs the question whether the weak moment in $LaMnO_3$ is due to the single ion crystal field interaction, or the antisymmetric D-M exchange. Both are possible in principle in perovskites with orthorhombic Pbnm symmetry [20]. By symmetry the D-M vector $\boldsymbol{\mathcal{D}}$ has to lie in the mirror plane at $z = 1/4$ mid way between the antiferromagnetically coupled Mn planes at $z = 0$ and $z = 1/2$. Since the sublattice moments are along b, it follows that the weak moment, which is due to $\mathcal{D}_a$, is along c.

Alternatively, the single ion anisotropy can also give a resultant moment along c in a A_y type antiferromagnet. One can see that the oxygen octahedron around the Mn ion is distorted (Fig. 8). The three O-Mn-O distances at 1.4 K are 0.197 nm along the c axis, 0.218 nm along the b axis and 0.191 nm along the a axis [21]. The principal long axes of the MnO_6 octahedron are all tilted by $\theta = 8°$ out of the ab plane. Their projection on the plane makes an angle $\phi = 35°$ with the b axis. One plane of the structure is shown in Figure 8. In the next manganese plane, the inclination is at $-8°$ because of the mirror symmetry, but the moments are oppositely directed, so that the weak components along c add (see Fig. 9).

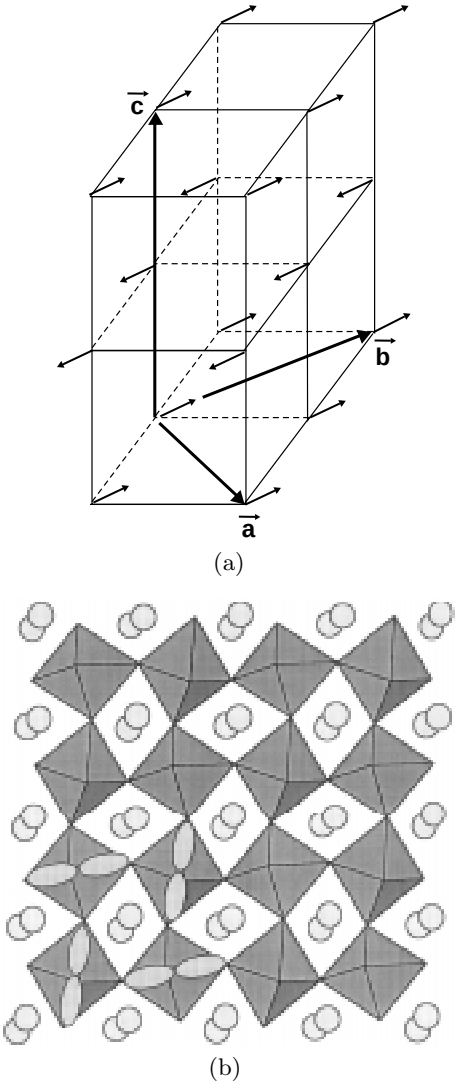

Fig. 8. (a) Scheme of the magnetic structure of $LaMnO_3$. Only Mn ions are represented. (b) Projection of the structure of $LaMnO_3$ in the ab plane. The MnO_6 octahedron are shown and the large circles represent La ions.

We can evaluate the weak moment expected from the crystal field interaction as follows. We consider a cubic crystal field plus a purely axial term of the form DS_z^2. The energy level scheme for a Mn^{3+} ion in a cubic crystal field (6-fold coordination) is shown in Figure 10.

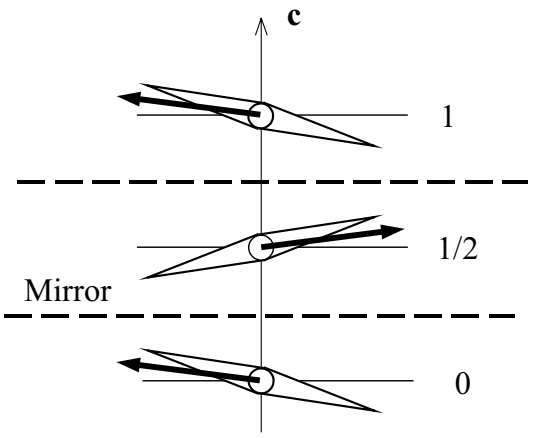

Fig. 9. Alternating antiferromagnetic *ab* planes. There are mirror plane at 1/4 and 3/4 perpendicular to the *c*-axes. The lozenges represent the direction of the local Jahn-Teller distortion which is also the local easy magnetisation axes. The bold arrows represent the magnetization direction in each plane. The competition between the antiferromagnetic exchange and the local anisotropy can account of some the alternating tilt of the magnetization direction which gives rise to a small resulting moment along *c* (see the text).

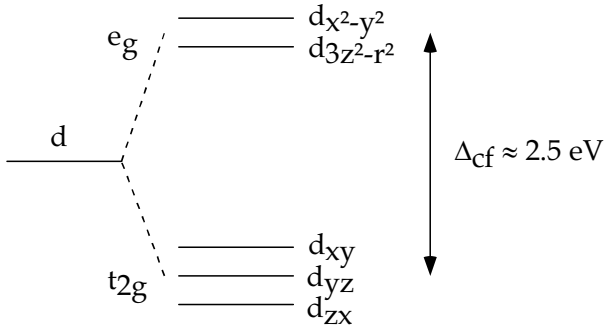

Fig. 10. Splitting of a Mn^{3+} ion *d* state in a cubic cristal field (six-fold coordination).

With a spin-orbit interaction of the form $\lambda \mathbf{L} \cdot \mathbf{S}$, it is possible to calculate the anisotropy constant $D = \lambda^2(\Lambda_\parallel - \Lambda_\perp)$ where $\Lambda_\parallel$ and $\Lambda_\perp$ are given by a second order perturbation calculation [22]. The calculation gives $D = 3\lambda^2/\Delta_{\rm cf}$ where λ is the spin-orbit coupling for Mn^{3+} ($= 127$ K [23]) and $\Delta_{\rm cf}$ is the separation of the e_g and t_{2g} levels ($\approx 25\,000$ K for $LaMnO_3$ [1]). Hence $D \approx 1.95$ K. Resolving the anisotropy along *a*, *b* and *c*, we find effective one-ion anisotropy constants D' of $D\cos\theta\sin\phi$, $D\cos\theta\cos\phi$ and $D\sin\theta$ respectively, *i.e.* $(0.57, 0.81, 0.14)D$.

It is also possible to calculate the anisotropy field knowing the exchange field and spin-flop field. The perpendicular susceptibility deduced from the high field measurements along *a* and *c* is $\chi_\perp = 9.5 \times 10^{-3}$. Let M_0 be the full magnetization of the material (4 $\mu_{\rm B}$/Mn), $M_0 = 0.608$ MA/m $= 0.76$ T. The intersublattice exchange field $H_{\rm E} = M_0/2\chi_\perp = 40$ T, in agreement with the value deduced from the exchange constant. The spin-flop field is related to the anisotropy and exchange fields by $H_{\rm sf} = \sqrt{H_{\rm A}^2 + 2H_{\rm A}H_{\rm E}}$ [24], so from $\mu_0 H_{\rm sf} = 17$ T, the value deduced for the anisotropy field is $\mu_0 H_{\rm A} = 3.8$ T. The corresponding anisotropy is then given by $K_{\rm A} = M_0 H_{\rm A} = 2.32 \times 10^6$ J/m^3 which corresponds to 10.2 K/Mn ion. The anisotropy field measures only the difference between the energy for the *b* and *c* directions *i.e.* $K_{\rm A} = 10.2\ {\rm K} = (0.81 - 0.14)DS_z^2$, $D = 3.8$ K (*c* is the next easiest antiferromagnetic axis after *b* because the net anisotropy when the moments lie along *a* is zero because of the zig-zag alignment of the octahedra (Fig. 7).

Inelastic neutron data from [4] have measured a spin wave gap corresponding to an effective value of $D' = 1.92$ K along *b*. The experimental value of the *D* coefficient is then $D'/0.81 = 2.4$ K. Independent confirmation of this gap is provided by the antiferromagnetic resonance frequency [25].

Even if we take the largest of these estimates of *D*, we will not succeed in explaining the magnitude of the weak moment. The anisotropy field along the *c*-axis for $D = 3.8$ K is 3.8 T. The antiferromagnetic exchange field is 40 T, which gives a net inclination of 0.8°, giving a weak moment of 0.06 $\mu_{\rm B}$ which is three times less than observed.

We therefore conclude that the D-M interaction is probably significant in $LaMnO_3$ and that the value of $\mathcal{D}$ needed to produce a weak moment of 0.12 $\mu_{\rm B}$ is 0.40 K. The canting angle due to the D-M interaction is given by $\tan\theta = \mathcal{D}/2J_2$. It may be noted that the weak moment in rare earth orthoferrites which have the same structure is of order 0.05 $\mu_{\rm B}$/Fe. There the effect is due to the D-M interaction because the single ion anisotropy is expected to be negligible for the S-state ion (Fe^{3+}). We have treated the two-ion anisotropy as a D-M phenomenological term. We however mention that there have been recent theoretical studies of the orbital ordering in manganite oxydes starting from microscopic Hamiltonians [26–29]. There is another possible explanation of the weak moment in $LaMnO_3$, which is non stoichiometry. If the compound is slightly cation-deficient, there is a concentration of holes which can give rise to double-exchange interactions. According to de Gennes [30] a canting of the antiferromagnetic sublattices then takes place which creates a weak moment proportional to the concentration *x*. More recently, the de Gennes theory has been criticized, and the likelihood of short range electron phase segregation has been emphasized [10]. In any case, comparing the weak moment measured in the $x = 0.06$ sample (0.40 $\mu_{\rm B}$/Mn) with that for the end member (0.18 $\mu_{\rm B}$/Mn) would lead us to a cation deficiency of $x \sim 0.03$ which is in excess of that expected for the $LaMnO_3$ crystal.

Finally we note that the sharp fall in χ' below $T_{\rm N}$ can be ascribed to the onset of coercivity. The losses are high around $T_{\rm N}$ because of the large domains arising from the feeble demagnetizing field in a weak ferromagnet. These domains are likely to give rise to large losses because large wall displacements mean that the walls may encounter high potentials barriers. The observed frequency dependence of the susceptibility reflects magnetization relaxation processes. We see in Figure 5 that the ratio between the amplitudes of the χ' and χ'' peaks for the

different frequencies is equal to 1/2 which suggests that the process is characterized by a narrow distribution in the relaxation time [31].

This work has been supported by the European TMR network OXSEN. We thank Dr. Gita Balakrishna for making available another $LaMnO_3$ crystal on which some additionnal measurements were made.

References

1. J.M.D. Coey, M. Viret, S. von Molnar, Adv. Phys. **48**, 2 (1999).
2. E. Wollan, W. Koehler, Phys. Rev. **100**, 545 (1995).
3. JBAA. Elemans, K.P. van Laar, K.R. van der Veen, B.O. Loopstra, J. Solid St. Chem. **3**, 238 (1971).
4. F. Moussa, M. Hennion, J. Rodrigez-Garvajal, H. Moudden, L. Pinsard, A. Revcolevschi, Phys. Rev. B **54**, 15149 (1996).
5. K. Hirota, N. Kaneko, A. Nishizawa, Y. Endoh, J. Phys. Soc. Jap. **65**, 3736-3739 (1996).
6. G. Matsumoto, J. Phys. Soc. Jap. **29**, 606 (1970).
7. T. Moriya, *Magnetism I (3)*, edited by Rado and Suhl (Academic Press, New York, 1963).
8. A.S. Borovik-Romanov, M.P. Orlova, Zh. Eksperim. I. Theor. Fiz. **36**, 766 (1959) [English transl.: Sov. Phys. - JETP **9**, 1204 (1957)].
9. C. Zener, Phys. Rev. **81**, 440 (1951).
10. S. von Molnar, J.M.D. Coey, Curr. Opin. in Solid State Mater. Sci. **3**, 171 (1998).
11. A. Revcolevschi, R. Collongues, C.R. Acad. Sci. (Paris) **266**, 1797 (1969).
12. J.P. Renard *et al.* (to be published).
13. Y.F. Popov, A.M. Kadomtseva, G.P. Vorob'ev, V. Yu. Ivanov, A.A. Mukhin, A.K. Zvezdin, A.M. Balbashov, J. Appl. Phys. **83**, 1760 (1998).
14. R.M. Bozorth, V. Kramer, J.P. Remeika, Phys. Rev. Lett. **1**, 1 (1958).
15. A.S. Borovik-Romanov, V.I. Ozhogin, Sov. Phys. JETP **12**, 18 (1961).
16. M. Matsuura, Y. Ajiro, T. Haseda, J. Phys. Soc. Jap. **26**, 665 (1969).
17. C. Dupas, J.P. Renard, Phys. Rev. B **18**, 401 (1978).
18. Y. Okuda, M. Matsuura, T. Haseda, J. Phys. Soc. Jap. **47**, 773 (1979).
19. H.A. Groenendijk A.J. van Duyneveldt, R.D. Willett, J.M.M.M. **15-18**, 1035 (1980).
20. R.M. Bozorth, Phys. Rev. Lett. **1**, 362 (1958).
21. L. Pinsard, Ph.D. thesis, University Paris XI, 1998; J. Rodriguez-Carvajal, M. Hennion, F. Moussa, A.H. Moudden, L. Pinsard, A. Revcolevschi, Phys. Rev. B **57**, R3189 (1998).
22. R.M. White, *Quantum theory of magnetism* (McGraw-Hill, New York, 1970) p. 57.
23. A. Abragam, B. Bleaney, *Résonance paramagnétique électronique des ions de transition* (Presses Univ. de France, Paris, 1971).
24. A.H. Morrish, *The Physical Principles of Magnetism* (Wiley & Sons, New York, 1966), pp. 475, 485. This formula is however only a first order approximation for a weak ferromagnet, for more details, see G. Cinader, Phys. Rev. **155**, 453 (1967).
25. V.Y. Ivanov, V.D. Travkin, A.A. Mukhin, S.P. Lebedev, A.A. Volkov, A. Pimenov, A. Loidl, A.M. Balbahov, A.V. Mozhaev, J. Appl. Phys. **83**, 7180 (1998).
26. D.I. Khomskii, G. Sawatzky, Solid State Comm. **102**, 87-99 (1997).
27. W. Koshibae, Y. Kawamura, S. Ishihara, S. Okamoto, J. Inoue, S. Maekawa, Physica B **237-238**, 48-50 (1997).
28. S. Ishihara, J. Inoue, S. Maekawa, Phys. Rev. B **55**, 8280 (1997).
29. L.F. Feiner, A.M. Oles, Phys. Rev. B **59**, 3295 (1999).
30. P.G. de Gennes, Phys. Rev. **118**, 141-154 (1960).
31. D.-X. Chen, V. Skumryev, J.M.D. Coey, Phys. Rev. B **53**, 15014 (1996).